Optical reflectance anisotropy of Ag(110): Evidence for contributions from surface-modified bulk band transitions

D. S. Martin,* N. P. Blanchard, and P. Weightman
Department of Physics and Surface Science Research Centre, University of Liverpool, L69 7ZE England, United Kingdom

D. S. Roseburgh and R. J. Cole
School of Physics, University of Edinburgh, EH9 3JZ Scotland, United Kingdom

J.-K. Hansen, J. Bremer, and O. Hunderi
Department of Physics, Norwegian University of Science and Technology, N-7034 Trondheim, Norway
(Received 28 May 2007; revised manuscript received 21 July 2007; published 6 September 2007)

We report measurements of the optical reflectance anisotropy (RA) of the Ag(110) surface as a function of temperature and we find evidence for contributions to the RA spectrum from bulk band transitions that are modified by the anisotropic (110) surface. A comparison is made between temperature-induced shifts in the energy of RA peaks and thermovariation optical spectroscopy results of the temperature dependence of transition energies between bands at the L symmetry point. A three phase model based on the energy derivative of the bulk dielectric function is found to simulate the RA response from well-ordered and Ar ion bombarded surfaces. We conclude that there is a general trend of surface-modified bulk band contributions to the RA response of the noble metal (110) surfaces.

DOI: 10.1103/PhysRevB.76.115403 PACS number(s): 73.20.At, 78.40.Kc, 78.68.+m

I. INTRODUCTION

Reflection anisotropy spectroscopy[1–3] (RAS) is a linear optical technique that probes the optical response of a surface as a function of photon energy by measuring Δr, the difference in normal incidence reflectance for orthogonal linear polarizations, normalized to the mean reflectance r. For Ag(110), the RAS is defined as

$$\frac{\Delta r}{r} = \frac{2(r_{[1\bar{1}0]} - r_{[001]})}{r_{[1\bar{1}0]} + r_{[001]}}, \tag{1}$$

where r_x represents the complex Fresnel reflection amplitude for x polarization. The RAS technique was originally developed as a real-time optical probe for use in semiconductor growth systems,[1] but over the past decade RAS has emerged as a powerful probe of metal surfaces and their interactions with adsorbates, allowing investigation of phenomena such as electronic surface states, reconstruction, surface alloying, and molecular assembly.[3]

In general, reflection anisotropy (RA) spectra of surfaces have proven to be rather complex, deriving from a combination of topological and electronic effects. The past decade has seen a concerted effort to develop the understanding of the technique by the study of model surfaces.[3] Recent RAS investigations of Cu(110) (Refs. 4 and 5) and Au(110) (Ref. 6) have found evidence that electronic bands of the bulk crystal modified in the vicinity of the anisotropic (110) surface contribute significantly to the RA spectrum. Similar contributions have previously been found in RAS studies of semiconductor surfaces.[7,8] For both Cu(110) and Au(110), transitions between bands near the Fermi level (E_F) at the L symmetry point are responsible for features in the RA spectra. The peaks observed at 4.25 and 4.9 eV in the RA spectrum of Cu(110) at room temperature were assigned to the optical transitions $E_F \rightarrow L_1^u$ and $L_2' \rightarrow L_1^u$, respectively.[4] For Au(110), the equivalent transitions have been assigned to the peaks observed in the room temperature RA spectrum at 3.52 and 4.50 eV, respectively.[6] The temperature dependence of the energy position of these RAS peaks, for both Cu and Au, was found to agree with the temperature dependence of the transition energies between the associated bands, as determined from thermovariation (ThV) optical spectroscopy.[9]

In the work presented here, we investigate whether similar contributions are present in the RA spectrum of the clean Ag(110) surface. We focus on investigating the RAS response of Ag(110) between 3.0 and 5.0 eV as a function of temperature. We compare temperature-induced shifts in the energy of RAS peaks to results of previous ThV,[9] thermoreflectance (ThR),[10] and ellipsometry[11] studies. We find evidence that bulk-related transitions similar to those observed in the RAS response of Cu(110) and Au(110) contribute a structure to the RA spectrum of Ag(110) and, thus, establish a general trend of "surface-modified bulk band contributions" to the RAS response of the noble metal (110) surfaces.

II. EXPERIMENT

The experiments were performed in an ultrahigh vacuum (UHV) environment with a base pressure in the 10^{-10} mbar region. Several Ag(110) single crystal specimens (SPL, Netherlands) were used that were aligned to better than $\sim 0.5°$ and mechanically polished to a mirror smooth finish before introduction into UHV. Clean Ag(110) surfaces were prepared in UHV by two methods. The first method involved repeated cycles of Ar ion bombardment (15 min, ~ 6 μA, 0.5 kV, and 300 K) and annealing to 830 K. The second method differed only in the annealing conditions of the final few (1–3) cycles, increasing the temperature to 1000 K. RA spectra obtained from each of the crystals were found to display the same features at the same photon energies. The

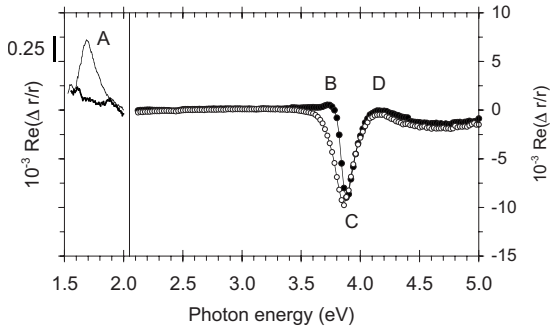

FIG. 1. RA spectra of clean Ag(110) at 300 K prepared by annealing at 830 K (filled circles) or 1000 K (open circles). The main features are labeled A–D. Peak A (thin line) and its absence at ~500 K (thick line) are shown on a different vertical scale for clarity.

temperature dependence of the energies of RAS features was reproducible, and small variations in the data obtained from different crystals are used in determining the errors. The temperature was measured using a thermocouple with a maximum uncertainty of ±20 K. Some variation in RAS intensity of the characteristic peaks of Ag(110) was observed between different crystals, and this variation is likely to be due to small differences in surface morphology and crystal orientation. The experiment monitoring the 1.7 eV RAS peak as a function of temperature was carried out at Trondheim, and all other experiments were performed in Liverpool.

Cleanliness was indicated by the presence of a RAS peak at the photon energy of 1.7 eV, involving transitions between surface states. X-ray photoelectron spectroscopy was used to confirm the absence of contaminants. Low energy electron diffraction (LEED) was used to monitor atomic order. For the Ar ion bombardment experiment, the clean well-ordered surface was bombarded at room temperature for the stated time using a beam energy of 0.5 kV and drain current ~6 μA.

A RA spectrometer having the design[1] of Aspnes *et al.* and utilizing a Xe photon source was coupled to the UHV chamber through a low-strain window. Experimental artifacts were removed from the spectra using a correction function obtained by measuring spectra with the specimen in two orthogonal positions. This correction function was a linear slope of gradient $\sim -1 \times 10^{-3}$ eV^{-1}. Spectra of the real part of the complex RA were obtained at the constant temperature indicated. Scanning tunneling microscopy (STM) was performed at room temperature in constant current mode using an Omicron STM. A tunneling current of 1 nA and bias voltages in the range from −0.5 to −1.0 V were used. STM tips were made from electrochemically etched tungsten wire.

III. RESULTS

A. Reflectance anisotropy spectrum of Ag(110) at room temperature

The RA spectrum of clean Ag(110) at 300 K, prepared by repeated cycles of ion bombardment at 300 K and annealing at 830 K, is shown by the filled circles in Fig. 1. The RAS profile is characterized by a peak at 1.7 eV (labeled A in Fig. 1), a small peak near 3.7 eV (B), a negative peak at near 3.9 eV (C), and a positive peak at ~4.1 eV (D). Previous RAS studies of the clean Ag(110) surface prepared in UHV[12–16] have reported a broadly similar RAS line shape in the 3–5 eV region, however, the RAS response in the region of peak B differs considerably from some surfaces exhibiting similarly clear (1×1) LEED patterns. The results of Stahrenberg *et al.*[15] showed an intense peak B [$\mathrm{Re}(\Delta r/r) \sim 30 \times 10^{-3}$], whereas Fernandez *et al.*[12] reported a spectrum with only a weak peak B [$\mathrm{Re}(\Delta r/r) \sim 1 \times 10^{-3}$]. Bremer *et al.*[16] offered the first insight into this variability by combining RAS and STM results to find out that the intensity of peak B is highly sensitive to surface morphology. A relatively intense peak B is observed for a rough morphology present on surfaces prepared using a limited number of cleaning cycles, whereas peak B is reduced significantly for a surface of well-ordered terraces terminated by monoatomic height steps of no preferred direction.

We note that the RA spectrum shown by the filled circles of Fig. 1 is very similar to that observed previously by Bremer *et al.*[16] In agreement with that work, our STM results show a well prepared surface consisting of flat terraces of widths ranging from ~5 to 100 nm and meandering steps. One notable difference is that on the crystal under study in the present STM work, although the steps meander, there is a tendency for an appreciable fraction of steps to show an alignment toward the $[1\bar{1}0]$ direction.

We find that performing a further few ion bombardment and/or annealing cycles with an increased annealing temperature of 1000 K produces steps that show a much greater tendency to align toward the $[1\bar{1}0]$ direction. STM results [Fig. 2(a)] show that the morphology of the surface consists of well-ordered terraces that are terminated by monoatomic height steps. Terrace widths in the [001] direction lie in the range ~5–100 nm; however, there is a distinct bias toward narrow (~5–10 nm) terrace widths and, therefore, a greater density of steps per unit area [Fig. 2(a)].

For surfaces prepared at 830 and 1000 K, step edge frizziness is observed at room temperature [Fig. 2(a)], indicating the mobility of adatoms on the surface. The open circles in Fig. 1 show the RAS profile observed from the surface prepared by final annealing at 1000 K. A shoulder is now observed at B and a small (0.02 eV) shift to lower energy is found for peaks C and D. The differences in the two RA spectra in Fig. 1 between 3 and 5 eV are, thus, attributed to the relatively small differences in surface morphology.

We note that RAS profiles exhibiting a peak at B may contribute to the line shape at peaks C and D, and that the "simplest" surface—both in terms of morphology and RAS response—is one that is prepared by annealing at 1000 K. Nonetheless, we have investigated the temperature dependence of the RAS response from surfaces prepared by annealing at 830 K (filled circles, Fig. 1) and 1000 K (open circles, Fig. 1), and find similar trends in their behavior with respect to temperature. We first discuss peak A and then report the results of the temperature dependence of the RAS peaks C and D.

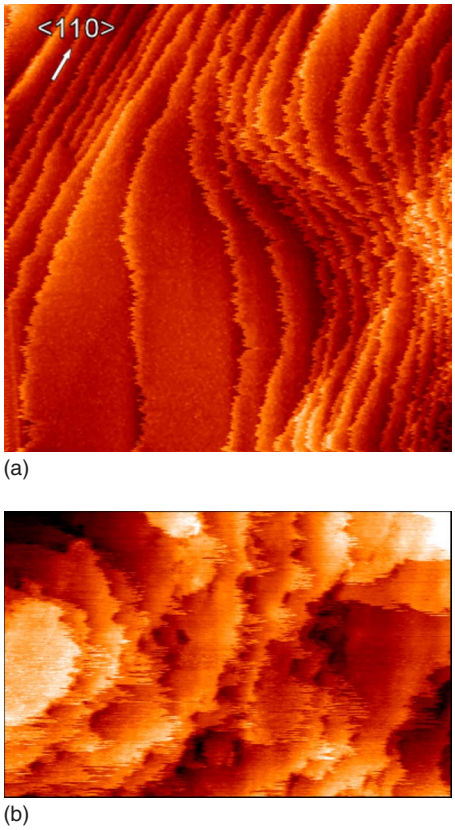

FIG. 2. (Color online) Room temperature STM data of the Ag(110) surface. Upper panel: clean and well ordered, prepared by annealing at 1000 K (200×200 nm^2). Lower panel: 42 min Ar ion bombarded surface (200×128 nm^2). Orientation is the same for both images.

B. Transitions between surface states: Peak A

It is known that peak A arises from transitions between surface states near E_F at the $\bar{Y}$ point of the surface Brillouin zone.[13,15] At room temperature, the occupied surface state resides at ~60 meV below E_F,[17,18] and the unoccupied surface state at ~1.6 eV above E_F.[18–20] Figure 3 shows in detail the behavior of RAS peak A with increasing temperature. We find that the intensity of peak A decreases with increasing temperature and becomes indistinguishable from the background profile at a temperature of 520 K (Fig. 3). Photoemission results[18] of the occupied surface state show a linear shift in the energy of the bottom of the band toward E_F between ~60 and 450 K. By extrapolation, this surface state band is predicted to cross E_F at a temperature of ~620 K.[18] A resonant enhancement of the second-harmonic generation signal of Ag(110) at 1.74 eV has been found due to a coupling with the transitions between the surface states at $\bar{Y}$,[21] and a reduction in the intensity of this signal with increasing temperature is observed, with the intensity approaching a background level near a temperature of ~500 K,[18,22] similar to our RAS results.

The energy position of peak A is found to shift linearly to lower energy between 310 and 420 K at a rate $\sim2.7\times10^{-4}$ eV/K (Fig. 3). This is comparable to the rate at which the energy of the occupied surface state shifts toward E_F with temperature, $\sim1.7\times10^{-4}$ eV/K.[18] Inverse photoemission measurements of the unoccupied state as a function of temperature would be desirable; however, to our knowledge no such work has been reported.

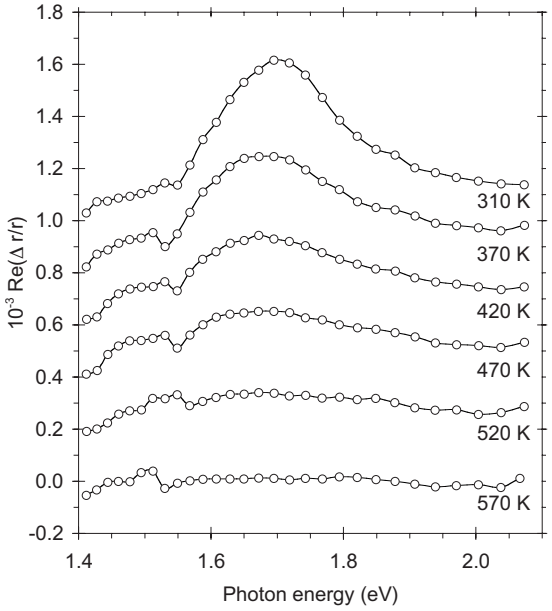

FIG. 3. RAS of Ag(110) peak A as a function of temperature. Each spectrum was recorded at the constant temperature stated. Spectra (apart from 570 K) are offset on the vertical axis for clarity.

C. Thermal behavior of peaks C and D

RA spectra measured as a function of temperature, using the surface prepared by annealing at 1000 K, are shown in Fig. 4. The temperature dependence of the energies of peaks C and D (for surfaces prepared at 830 and 1000 K) is plotted in Fig. 5. The peak positions were measured from a series of RA spectra, some of which are shown in Fig. 4. The data in Fig. 5 show a shift in peak position to lower photon energy with increasing temperature.

The RA spectra of Ag are reminiscent of spectra measured using ThV spectroscopy,[9] a technique that yields $\Delta\epsilon_b''/\Delta T$, the change in the imaginary part of the bulk dielectric function per unit change in temperature. In general, peaks in ϵ_b'' (we use the notation $\epsilon=\epsilon'+i\epsilon''$) arise from interband transitions at critical points and so ThV spectroscopy can reveal the T dependence of optical gaps. In the range 400–750 K, the Ag ThV data of Winsemius *et al.*[9] show a linear reduction of the optical gaps around 4 eV with T, having a gradient of -8.5×10^{-4} eV/K. Shifts in transition energy became more pronounced at higher temperature.

In the range 300–830 K, we find that the positions of the RAS peaks in Fig. 5 vary linearly with T, with the gradients shown in Table I. Similar data (also shown in Fig. 5) were obtained from the surface prepared at 830 K, and those gradients are presented in brackets in Table I. The table shows that the values deduced from RAS are consistent with the gradients observed using ThV spectroscopy,[9] ThR

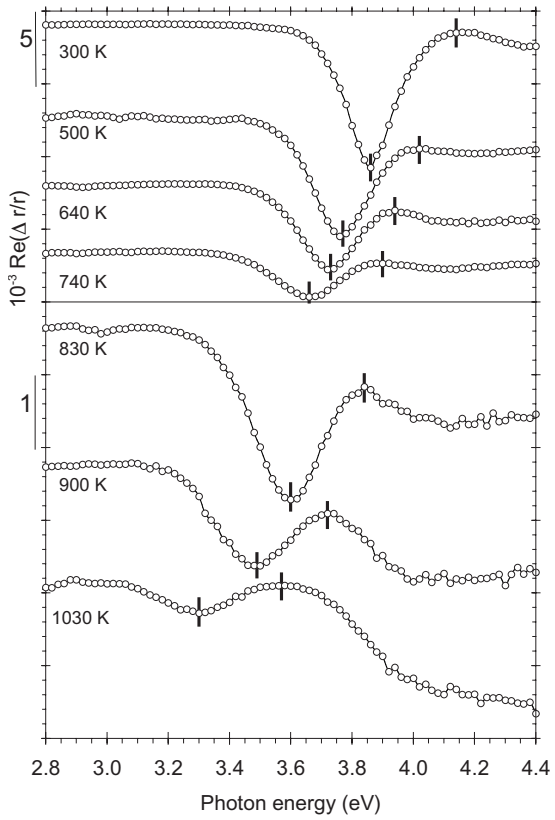

FIG. 4. RAS of Ag(110) peaks C and D as a function of temperature. Each spectrum was recorded at the constant temperature stated. Spectra are offset on the vertical scale for clarity.

spectroscopy,[10] and ellipsometry[11] despite the quite different measurement techniques employed.

D. Effects of ion bombardment

The effects of Ar ion bombardment at room temperature on the RA response of Ag(110) are shown in Fig. 6. Similar results are obtained using starting surfaces prepared at 830 or 1000 K. It is clear from the figure that ion bombardment causes substantial modification of the RAS signature. With increasing bombardment time, a near reversal of the RA spectrum is observed, with peaks C and D appearing to change sign (Fig. 6). The RA response at ~3.95 eV remains relatively insensitive to ion bombardment. The largest change to the RA spectrum was observed following an ion bombardment time of 42 min, with further bombardment time producing no significant change from this profile.

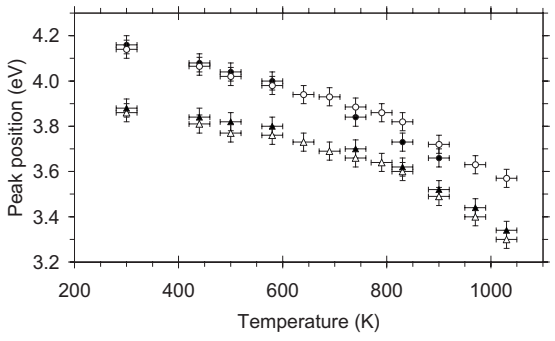

FIG. 5. RAS peak position as a function of temperature for peak C (triangles) and peak D (circles). Filled and open symbols refer to the surfaces prepared at 830 and 1000 K, respectively. Peak positions were measured from RA spectra recorded while the crystal was held at the particular temperature.

TABLE I. Temperature dependence of RAS peaks C and D (values before and in brackets refer to the surface prepared at 1000 and 830 K, respectively), their assignments to transitions involving L bands, and the corresponding shifts of these transitions as measured by other spectroscopic techniques. All values are in units of 10^{-4} eV/K.

RAS peak energy (300 K)	3.86 eV (C)	4.14 eV (D)
Assignment	$E_F \rightarrow L_1^u$	$L_2' \rightarrow L_1^u$
Shifts:		
RAS (300–830 K)	−4.8 (−4.8)	−5.9 (−8.1)
ThV (300–740 K)[a]	−8.5	−8.5
ThR (400–800 K)[b]	−6.5	−6.0
Im(ϵ_2) (298–773 K)[c]	−6.0	

[a]Reference 9.
[b]Reference 10.
[c]Reference 11.

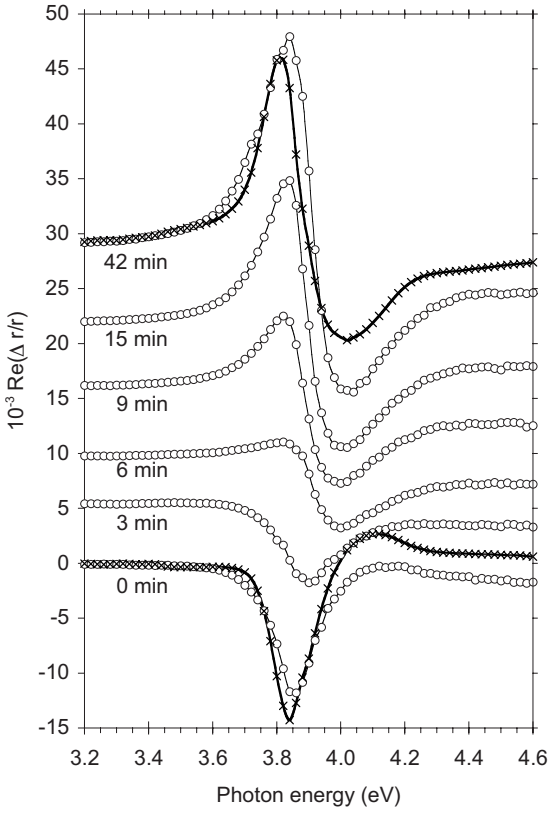

FIG. 6. The effect on the RA response of Ag(110) upon increasing Ar ion bombardment time. Spectra (apart from 0 min) are offset on the vertical axis for clarity. The solid lines show the simulated RA spectra of well-ordered (annealed at 1000 K) and 42 min bombarded Ag(110).

The STM image of Fig. 2(b) shows the surface following an ion bombardment of 42 min and subsequent annealing at room temperature for approximately 60 min. Figure 2(b) shows that there is a larger proportion of terraces having larger widths in the [001] direction compared to that on the surface before ion bombardment [Fig. 2(a)]. The steps meander to a much greater extent and step edge profiles appear more jagged following bombardment, with step edge frizziness observed, compared to that before bombardment [Figs. 2(a) and 2(b)]. A few vacancy aggregates of monoatomic depth are observed on the terraces following ion bombardment [small dark holes, Fig. 2(b)]. The results shown in Fig. 6 demonstrate the high sensitivity of RAS to the morphology of the surface layer. RAS performed on the surface of Fig. 2(b) following completion of STM imaging showed no significant difference from the spectrum obtained immediately after the bombardment. This observation suggests that the morphology after 60 min may be similar to that existing immediately after the bombardment.

IV. DISCUSSION

A. Three-phase derivative model

Having an isotropic bulk optical response, the reflectance anisotropy of Ag(110) must derive from an anisotropic surface region. The "three-phase model"[23,24] assumes that dielectric properties vary abruptly at the interfaces between vacuum, surface layer, and substrate. In the thin film limit where the surface layer thickness d is much less than the wavelength of light λ, we have

$$\frac{\Delta r}{r} = -\frac{4\pi i d}{\lambda}\frac{\Delta \epsilon_s}{\epsilon_b - 1}, \tag{2}$$

where $\Delta\epsilon_s$ is the dielectric anisotropy in the surface layer. The real and imaginary parts of $(1-\epsilon_b)^{-1}$, denoted $A(E)$ and $B(E)$, respectively, where E is energy, are shown in Fig. 7 for each of the noble metals. Dielectric data for our simulations are obtained from Cu,[25] Ag,[25] and Au.[26] It can be seen that in the case of Ag, these functions vary strongly at around 3.9 eV, indicating a strong substrate influence on the RA spectra of Ag(110).

In contrast, the $A(E)$ and $B(E)$ functions of Au and Cu do not exhibit very strong structure above their $d \rightarrow E_F$ thresholds, yet the RA spectra of Cu(110) and Au(110) both exhibit distinct features at photon energies above these thresholds corresponding to bulk critical point optical gaps. This has been explained using the "derivative model" in which the surface is assumed to perturb the electronic structure of the subsurface region, modifying the energies E_g and linewidths Γ of interband transitions at critical points. For (110) surfaces, there are different energy and broadening shifts for $[1\bar{1}0]$ and [001] polarized light, leading to

$$\frac{\Delta r}{r} = -\frac{4\pi i d}{\lambda}\frac{(\Delta E_g + i\Delta\Gamma)}{\epsilon_b - 1}\frac{d\epsilon_b}{dE}, \tag{3}$$

where ΔE_g and $\Delta\Gamma$ are the differences in gap energies and linewidths for the two polarizations. The real part of $\Delta r/r$ then takes the form

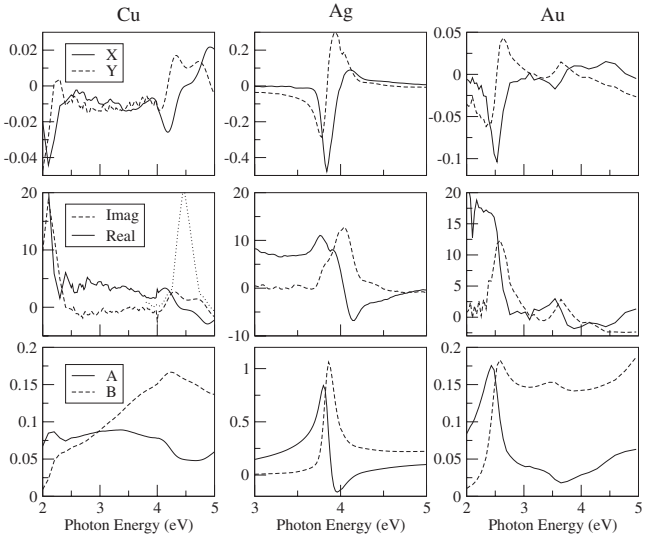

FIG. 7. Dielectric data for Cu, Ag, and Au. The lower panels show the $A(E)$ and $B(E)$ functions, the middle panels show the real and imaginary parts of the energy derivative of the bulk dielectric functions (Refs. 25 and 26), while the upper panels show the $X(E)$ and $Y(E)$ functions defined by Eqs. (5) and (6).

$$\Re\left[\frac{\Delta r}{r}\right] = X(E)\Delta E_g + Y(E)\Delta\Gamma, \tag{4}$$

where

$$X(E) = -\frac{4\pi d}{\lambda}\left[B(E)\frac{d\epsilon_b'}{dE} + A(E)\frac{d\epsilon_b''}{dE}\right] \tag{5}$$

and

$$Y(E) = \frac{4\pi d}{\lambda}\left[B(E)\frac{d\epsilon_b''}{dE} - A(E)\frac{d\epsilon_b'}{dE}\right]. \tag{6}$$

Thus "bulk features" can enter the noble metal RA spectra through either the numerator or denominator of the right hand side of Eq. (2). Before applying this model to simulate the RA response of Ag(110), we pause briefly to consider the line shape of the dielectric functions [and hence the $X(E)$ and $Y(E)$ functions] of the noble metals.

B. Bulk derivative spectra

Derivatives of the dielectric functions of the noble metals are shown in Fig. 7. It is evident that these profiles for Au and Cu show similarities. In each case, the low energy peak in $d\epsilon_b''/dE$ (at 2.1 eV for Cu and 2.5 eV for Au) has been assigned to the $L_3 \rightarrow L_2'(E_F)$ absorption edge, while the features for higher energy have been assigned to transitions between bands 6 and 7 in the vicinity of the L point. The $L_2'(E_F) \rightarrow L_1$ edge gives rise to a peak in $d\epsilon_b''/dE$ (at 3.6 eV for Au and 4.3 eV for Cu), while the $L_2' \rightarrow L_1$ transition creates an oscillatory structure (centered on 4.2 eV for Au and 4.8 eV for Cu). For both Cu and Au, the bulk derivative spectra closely resemble the corresponding ThV spectra. The relative magnitudes of these spectra imply a variation of the

$L_2' \rightarrow L_1$ gap of $\sim 5 \times 10^{-4}$ eV/K in each case, and ThV measurements[9] at elevated temperature confirm this estimate.

Turning to Ag, we may expect similar behavior to that of Au and Cu, except perhaps with the d to E_F transitions moved further toward the UV. Such behavior is simulated by the dotted curve in Fig. 7 (Cu, middle panel), which has been obtained by shifting the $L_3 \rightarrow L_2'(E_F)$ peak in the $d\epsilon_b''/dE$ spectrum of Cu by 2.4 eV so that it overlaps the structure attributed to the L_2 to L_1 transitions. The resulting spectrum does, indeed, resemble the $d\epsilon_b''/dE$ spectrum of Ag (middle panel, Fig. 7) although it is generally believed that this d to Fermi level peak has contributions arising from transitions in extended regions of the Brillouin zone of Ag.[9,11,27] Assuming that the dotted curve in Fig. 7 gives correct insight into the derivative spectrum of Ag, we deduce the energies of the $d \rightarrow E_F$, $L_2'(E_F) \rightarrow L_1$ and $L_2' \rightarrow L_1$ transitions at room temperature to be 4.02, 3.82, and 4.46 eV, respectively, while the values deduced by Winsemius *et al.*[9] from Ag ThV data were 3.98, 3.86, and 4.11 eV. Two reasons for the unsatisfactory agreement on the value of the $L_2' \rightarrow L_1$ transition are plausible. Firstly, the analogy between the dotted curve in Fig. 7 and the $d\epsilon_b''/dE$ spectrum of Ag may not be valid. Secondly, the discrepancy may be due to the fundamentally different optical properties of the specimens used in the two studies; the Ag ThV spectrum (obtained from an evaporated thin film[9]) does not resemble the $d\epsilon_b''/dE$ spectrum in Fig. 7 (measured from a single crystal[25]) in the 4.0–4.5 eV region. Effects on ϵ_b due to specimen quality and preparation have been noted previously.[28,29] In principle, this question could be resolved by an *ab initio* electronic structure calculation for Ag. Results of such a calculation, performed at the GW level, have recently been shown[30] to give a good description of the main interband threshold, but do not appear to give a precise description of the reflectivity and dielectric function of Ag in the 4–5 eV region. Several first principles calculations of Ag (Refs. 30–32) have indicated that transitions between bands which occur over a number of k points may contribute to the RAS of Ag(110). A complete description of the origin of the features observed experimentally in the 4.2–5.0 eV region has yet to be achieved.

C. Reflectance anisotropy spectra

The $X(E)$ and $Y(E)$ functions for Ag, obtained using the value $d=1$ nm and the ϵ_b data of Stahrenberg *et al.*[25] for a clean single crystal Ag(110) at room temperature, are shown in Fig. 7. It can be seen that the $X(E)$ function resembles the room temperature RA spectrum of Ag(110). The intense feature in $X(E)$ corresponding to peak C in the RA spectrum is determined primarily by the peak in the $B(E)$ function of Ag. The weak feature at 4.12 eV originates from the negative component of the oscillation in $d\epsilon_b'/dE$ centered on 4.0 eV and derived from d to Fermi level transitions.

The observed similarity between $X(E)$ and the well-ordered room temperature RA spectrum suggests that ΔE_g in Eq. (4) dominates the $\Delta\Gamma$ term. This result is in agreement with other simulations based on similar two and three layer models.[12,16] We find that the RA spectrum is well simulated using the parameters $\Delta E_g=0.03$ eV and $\Delta\Gamma=0.00$ eV, and the result of the simulation is shown by the lower solid line in Fig. 6. Similarly, the optical anisotropy of the Cu(110) surface around 4 eV is well described by Eq. (4) with a dominant ΔE_g term. This result has been interpreted[4] in terms of the reduced coordination of atoms on Cu(110) terraces relative to the bulk. Band narrowing leads to an energy shift to preserve the occupancy of the band, leading to a modification of the E_g gap parameters for optical transitions.[33,34] The structural anisotropy of the (110) surface causes different band narrowing along [001] and $[1\bar{1}0]$, and hence, ΔE_g is nonzero. Further evidence for the importance of surface atomic coordination in the interpretation of RAS data is provided by the recent RAS study of vicinal Cu(111) surfaces by Baumberger *et al.*[35] It was found that for a RAS peak observed at 4.3 eV deriving from the presence of steps, the sign of the peak was determined by the atomic coordination at step edges.[35]

We find that the RA spectrum obtained following ion bombardment for 42 min can be simulated well using the three-phase model with parameters $\Delta E_g=-0.03$ eV and $\Delta\Gamma=-0.03$ eV (upper solid line, Fig. 6). Both parameters have the same magnitude, and hence, an equal weighting of $X(E)$ and $Y(E)$ is used in Eq. (4). The three-phase model has been found to simulate the RA response of Ar ion bombarded Au(110) (Ref. 6) and Cu(110),[36] and we found that equal magnitudes of ΔE_g and $\Delta\Gamma$ produces the best fit for both ion bombarded Ag(110) and Cu(110). However, for the ion bombarded Au(110) surface,[6] we deduced that $|\Delta\Gamma|$ dominates $|\Delta E_g|$. In this context, RAS of ion bombarded Au(110) is then different from those of ion bombarded Cu(110) and Ag(110). This difference coincides with a difference in surface morphology: Cu(110) (Ref. 36) and Ag(110) (Fig. 2) maintain flat terraces after the bombardment, whereas Au(110) shows an undulating morphology of disordered (1×2) structure with no equivalent large terrace structures.[5]

The assignment of the RA response in these energy regions to surface-modified bulk bands implies that these bands must be sensitive to the effects of Ar ion bombardment, which includes the creation of vacancies, vacancy aggregates, and a change in the terraces and step morphology, indicated by Figs. 2(a) and 2(b). We speculate that these changes in the surface layer introduce an increased broadening of the transitions $E_F \rightarrow L_1$ and $L_2' \rightarrow L_1$, with the $|\Delta\Gamma|$ term in Eq. (4) becoming nonzero for ion bombarded surfaces. The same energy region has been found to be sensitive to biomolecular adsorption.[37] Thus, we anticipate that the interpretation of the RAS response of the clean surface will also aid in the interpretation of molecular adsorption and other complex systems involving Ag surfaces.

V. CONCLUSION

We have investigated the temperature dependence of the optical reflectance anisotropy of the Ag(110) surface and found evidence for contributions from bulk band transitions at L that are modified by the anisotropic surface. These contributions result in RAS peaks observed at room temperature at 3.86 and 4.14 eV. Analogous observations in the RA

spectrum of Cu(110) and Au(110) have been attributed to *d* band narrowing at the surface due to the reduced coordination of surface sites. We conclude that there is a general trend of surface-modified bulk band contributions to the RA response of the noble metal (110) surfaces.

ACKNOWLEDGMENTS

The authors acknowledge the financial support of the UK EPSRC. D.S.M. thanks N. Esser and Th. Herrmann for providing dielectric function data of Ag and Cu from Ref. 25.

*david.martin@liverpool.ac.uk; www.liv.ac.uk/~davidm

[1] D. E. Aspnes, J. P. Harbison, A. A. Studna, and L. T. Florez, J. Vac. Sci. Technol. A **6**, 1327 (1988).
[2] D. S. Martin and P. Weightman, Thin Solid Films **455-456**, 752 (2004).
[3] P. Weightman, D. S. Martin, R. J. Cole, and T. Farrell, Rep. Prog. Phys. **68**, 1251 (2005).
[4] L. D. Sun, M. Hohage, P. Zeppenfeld, R. E. Balderas-Navarro, and K. Hingerl, Surf. Sci. **527**, L184 (2003).
[5] D. S. Martin, N. P. Blanchard, and P. Weightman, Surf. Sci. **532-535**, 1 (2003).
[6] D. S. Martin, R. J. Cole, N. P. Blanchard, G. E. Isted, D. S. Roseburgh, and P. Weightman, J. Phys.: Condens. Matter **16**, S4375 (2004).
[7] R. Del Sole and G. Onida, Phys. Rev. B **60**, 5523 (1999).
[8] W. G. Schmidt, N. Esser, A. M. Frisch, P. Vogt, J. Bernholc, F. Bechstedt, M. Zorn, Th. Hannappel, S. Visbeck, F. Willig, and W. Richter, Phys. Rev. B **61**, R16335 (2000).
[9] P. Winsemius, F. F. van Kampen, H. P. Lengkeek, and C. G. van Went, J. Phys. F: Met. Phys. **6**, 1583 (1976).
[10] E. Colavita, S. Modesti, and R. Rosei, Phys. Rev. B **14**, 3415 (1976).
[11] H. G. Liljenvall and A. G. Mathewson, J. Phys. C **3**, S341 (1970).
[12] V. Fernandez, D. Pahlke, N. Esser, K. Stahrenberg, O. Hunderi, A. M. Bradshaw, and W. Richter, Surf. Sci. **377-379**, 388 (1997).
[13] J.-K. Hansen, J. Bremer, and O. Hunderi, Surf. Sci. **418**, L58 (1998).
[14] J.-K. Hansen, J. Bremer, and O. Hunderi, Phys. Status Solidi A **170**, 271 (1998).
[15] K. Stahrenberg, T. Herrmann, N. Esser, J. Sahm, W. Richter, S. V. Hoffmann, and Ph. Hofmann, Phys. Rev. B **58**, R10207 (1998); **61**, 13287 (2000).
[16] J. Bremer, J.-K. Hansen, K. Stahrenberg, and T. Worren, Surf. Sci. **459**, 39 (2000).
[17] R. A. Bartynski and T. Gustafsson, Phys. Rev. B **33**, 6588 (1986).
[18] A. Gerlach, G. Meister, R. Matzdorf, and A. Goldmann, Surf. Sci. **443**, 221 (1999).
[19] W. Altmann, V. Dose, and A. Goldmann, Z. Phys. B: Condens. Matter **65**, 171 (1986).
[20] A. Goldmann, V. Dose, and G. Borstel, Phys. Rev. B **32**, 1971 (1985).
[21] L. E. Urbach, K. L. Percival, J. M. Hicks, E. W. Plummer, and H.-L. Dai, Phys. Rev. B **45**, 3769 (1992).
[22] J. M. Hicks, in *Laser Spectroscopy and Photochemistry on Metal Surfaces*, edited by H.-L. Dai and W. Ho (World Scientific, Singapore, 1995), p. 606.
[23] J. D. E. McIntyre and D. E. Aspnes, Surf. Sci. **24**, 417 (1971).
[24] U. Rossow, L. Mantese, and D. E. Aspnes, J. Vac. Sci. Technol. B **14**, 3070 (1996).
[25] K. Stahrenberg, Th. Herrmann, K. Wilmers, N. Esser, W. Richter, and M. J. G. Lee, Phys. Rev. B **64**, 115111 (2001).
[26] N. P. Blanchard, C. Smith, D. S. Martin, D. J. Hayton, T. E. Jenkins, and P. Weightman, Phys. Status Solidi C **0**, 2931 (2003).
[27] R. Lässer, N. V. Smith, and R. L. Benbow, Phys. Rev. B **24**, 1895 (1981).
[28] P. Winsemius, H. P. Lengkeek, and F. F. Van Kampen, Physica B & C **79**, 529 (1975).
[29] D. E. Aspnes, E. Kinsbron, and D. D. Bacon, Phys. Rev. B **21**, 3290 (1980).
[30] A. Marini, R. Del Sole, and G. Onida, Phys. Rev. B **66**, 115101 (2002).
[31] P. Monachesi, M. Palummo, R. Del Sole, R. Ahuja, and O. Eriksson, Phys. Rev. B **64**, 115421 (2001).
[32] S. Bouarab, M. Mebarki, A. Ziane, and M. A. Khan, Phys. Rev. B **63**, 195409 (2001).
[33] P. H. Citrin, G. K. Wertheim, and Y. Baer, Phys. Rev. B **27**, 3160 (1983).
[34] P. H. Citrin and G. K. Wertheim, Phys. Rev. B **27**, 3176 (1983).
[35] F. Baumberger, Th. Herrmann, A. Kara, S. Stolbov, N. Esser, T. S. Rahman, J. Osterwalder, W. Richter, and T. Greber, Phys. Rev. Lett. **90**, 177402 (2003).
[36] D. S. Martin, R. J. Cole, and P. Weightman, Phys. Rev. B **72**, 035408 (2005).
[37] D. S. Martin, G. E. Isted, R. J. Cole, and P. Weightman, Phys. Status Solidi C **2**, 4043 (2005).